ELSEVIER

Journal of Nuclear Materials 313–316 (2003) 204–208

journal of nuclear materials

www.elsevier.com/locate/jnucmat

Blister formation in tungsten by hydrogen and carbon mixed ion beam irradiation

T. Shimada [a,*], H. Kikuchi [a], Y. Ueda [a], A. Sagara [b], M. Nishikawa [a]

[a] *Department of Electronic, Information Systems, and Energy Engineering, Graduate School of engineering, Osaka University, 2-1 Yamada-Oka, Suita, Osaka 565-0871, Japan*

[b] *National Institute for Fusion Science, Toki 509-5292, Japan*

Abstract

Blister formation in tungsten has been studied by mixed carbon and hydrogen ion beam irradiation. The beam ion energies were 1.0 keV and 300 eV, and the fluence was in the range of 10^{24}–10^{25} ions m^{-2}. It was found that a little amount of carbon impurity in the beam affected blister formation. A large number of blisters with various sizes were observed on the surface of tungsten at 653 K when the carbon concentration was more than 0.35%. When the carbon concentration was 0.11%, no blisters larger than 1.0 μm were observed. When the carbon concentration was 2.35%, a carbon layer developed on the tungsten surface, and again, no blisters were observed. The effect of target temperature on blister formation was also investigated: the sizes and numbers of the blisters were the largest when the tungsten was irradiated at 653 K; when the sample was irradiated at 388 or 873 K, no blisters larger than 1.0 μm were observed.

PACS: 52.40.H

Keywords: Blistering; Carbon impurity; Tungsten; Mixed ion beam irradiation; PFM

1. Introduction

International thermonuclear experimental reactor (ITER) will use various kinds of PFM. Current plans call for beryllium on the first walls and startup limiter, and carbon and tungsten in the divertors [1].

It is expected that the tungsten will be irradiated with carbon and oxygen impurity particles, as well as the deuterium and tritium fuel ions, if the divertor PFM is a mix of carbon and tungsten. This will affect surface erosion both physically or chemically.

For example, a very small amount of carbon in the plasma enhances sputtering erosion of tungsten, and if the carbon concentration exceeds the critical value, net carbon deposition takes place, protecting the tungsten surface from sputtering erosion [2,3]. The critical level is several percent, depending on the ion energy.

Carbon impurities in the plasma also affect surface deformation such as blister formation. Studies of pure hydrogen (or deuterium) irradiation into tungsten have been performed with ion beams and plasma simulators [4–7]. These studies showed that blisters of up to 50 μm in diameter were formed due to hydrogen diffusion beyond the ion range, followed by trapping at vacancies, dislocations, voids, or grain boundaries. However, there is little data regarding the effects of impurities on blister formation [8]. Intensive studies focusing on this issue are needed to make a complete evaluation of tungsten's performance as a PFM.

This study is an investigation of the effects of carbon impurities on blister formation in tungsten by mixed carbon and hydrogen ion beam irradiation.

* Corresponding author. Tel.: +81-6 6877 5111x3675; fax: +81-6 6879 7867.

E-mail address: tshimada@ppl.eng.osaka-u.ac.jp (T. Shimada).

0022-3115/03/$ - see front matter
PII: S0022-3115(02)01447-2

2. Experiment

The experiments were performed in the high flux ion beam test device (HiFIT) [9–11]. A schematic view of this device is given in Fig. 1. HiFIT consists of a 2.45 GHz ECR ion source, triode spherical electrodes, a beam chamber, a sample irradiation chamber, an ion mass spectrometer and a thermal desorption (TDS) chamber. The beam flux is large enough to simulate PWI at the first wall, divertor sidewall and dome. For hydrogen beam, flux of 3.6×10^{21} $m^{-2} s^{-1}$ is obtained at the beam energy of 3.0 keV (H_3^+ dominant); flux of 4.1×10^{20} $m^{-2} s^{-1}$ is obtained at the beam energy of 300 eV by applying high deceleration voltage to an intermediate electrode. These fluxes are much higher than conventional mass-analyzed ion beam devices, which usually have fluxes of $<10^{20}$ $m^{-2} s^{-1}$.

A sample was positioned at the focal point of the beam in the sample irradiation chamber. All results were obtained using sintered polycrystalline tungsten samples of 99.95 wt% purity. The samples were 0.5 mm in thickness, 10×20 mm in size, polished to the mirror finish, and not annealed. The irradiation area was defined by a ϕ 3 mm aperture in front of the samples. The usual beam energy, flux, and fluence were 1.0 keV, $\sim 4.0 \times 10^{20}$ $m^{-2} s^{-1}$, and 10^{24}–10^{25} m^{-2}, respectively. Samples were heated to 388–873 K with an IR-heater and the sample temperature was measured using a thermocouple which was inserted into a center point of a copper holder. The copper holder was attached to the sample material (see Fig. 1).

Before and after irradiating a sample, the ion beam mass spectrum was measured in order to estimate the ratio of ion species, particularly the carbon impurity concentration. The ratio of ion species depends on plasma density and gas pressure, and not on beam energy. It is no problem that beam energy setting for the mass spectrum measurement is different from that for beam irradiation to the sample materials. Setting beam energy of 3.0 keV is more suitable to measure the mass spectrum than that of 1.0 keV. Typical mass spectrum of the mixed beam is shown in Fig. 2.

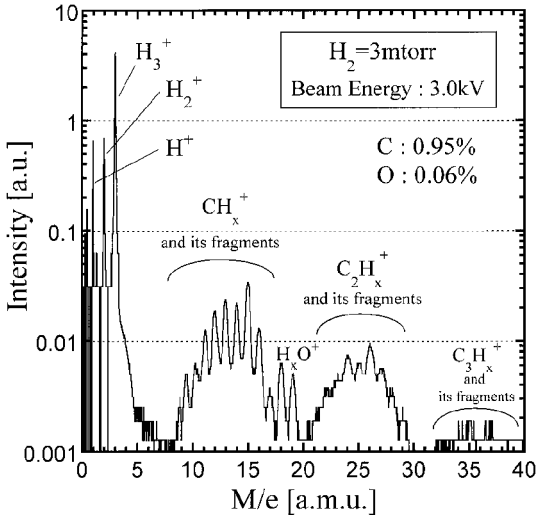

Fig. 2. Mass spectrum for carbon and hydrogen mixed ion beam.

From Fig. 2, hydrogen atoms were observed as H_3^+, H_2^+, and H^+. H_3^+ was mainly contained in the beam (70–80%). Carbon atoms were observed as CH_x^+ molecular ions and $C_2H_x^+$ molecular ions. The former was dominant. Molecular ions of $C_3H_x^+$ were so rare that they were neglected for impurity concentration estimation. These ions are subject to dissociation and neutralization in the beam transport region through the collisions with ambient gas molecules (mainly H_2). Some fragmented ions from CH_x^+ and $C_2H_x^+$ by the dissociation process were observed between the mass number from 9.0 to 12.0, and from 21.0 to 24.0. The observed mass number

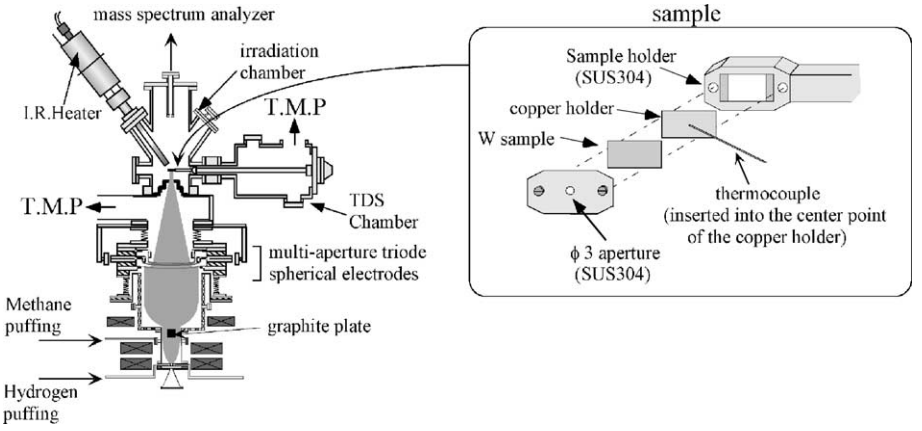

Fig. 1. Schematic view of the high flux ion beam test device (HiFIT) and the sample holder.

of fragmented ions is expressed as M_f^2/M_I, where M_f and M_I denote mass number of fragmented ions and extracted ions from the ion source, respectively. From this calculation, for example, it is known that the observed mass of 9.6 and 10.29 correspond to C^+ ions fragmented from CH_3^+ and CH_2^+, respectively, and that the observed mass of 21.33 and 23.04 correspond to C_2^+ ions fragmented from $C_2H_3^+$ and C_2H^+, respectively. The carbon concentration in the beam can be controlled from 0.11% to roughly 10% by changing the amount and size of graphite plates put inside the ion source and the flow rate of the puffed methane gas. There was less than 0.10% oxygen as H_xO^+ ions in the beam. Other species were less than the detection limit (0.01%).

3. Results and discussion

3.1. Effect of carbon concentration in the beam

Fig. 3 shows SEM micrographs of the irradiated regions of tungsten samples, after implantation at 1.0 keV and 653 K. In this experiment the carbon concentration in the ion beam was varied from 0.11% to 2.35%. When the carbon concentration exceeded 0.35%, many blisters of various sizes were formed on the surface (Fig. 3(b) and (c)). As the carbon concentration was increased, the number and size of the blisters formed increased. From cross-sectional SEM, blisters were observed at the depth of the order of micrometers, which is much deeper than ion range of hydrogen (around 10 nm). Surface erosion was also observed, and attributed to the carbon ions primarily. When the carbon concentration was 0.95%, the tungsten surface was eroded by about 200 nm, as indicated by a surface profile-scanning device (Dektak^3, Veeco Co.). Blisters formed on the surface at fluence of $>1.0 \times 10^{24}$ m^{-2}. Blisters were observed even with the beam energy reduced to 300 eV with the carbon concentration of 0.80% and at a beam fluence of 3.4×10^{24} m^{-2}. But the number of blisters formed was lower than the case of 1.0 keV irradiation with the carbon concentration of 0.70% and at a beam fluence of 2.8×10^{24} m^{-2}.

In the case of a carbon concentration of 0.11% (Fig. 3(a)), there was only erosion by about 30 nm. Blisters of sizes greater than 1.0 μm were not observed under this condition. When the carbon concentration was 2.35% (Fig. 3(d)), blisters were not observed after the beam irradiation at fluence of 3.6×10^{24} m^{-2} because a carbon layer built up to a thickness of about 220 nm. Krieger and Roth [12] evaluated the erosion of tungsten and the deposition and re-erosion of carbon. Referring their calculation, for a mixed ion beam of hydrogen (333 eV H) and carbon (1.0 keV C), the critical carbon concentration over which carbon net deposition takes place is 1.50%. This is roughly in agreement with the above experimental results.

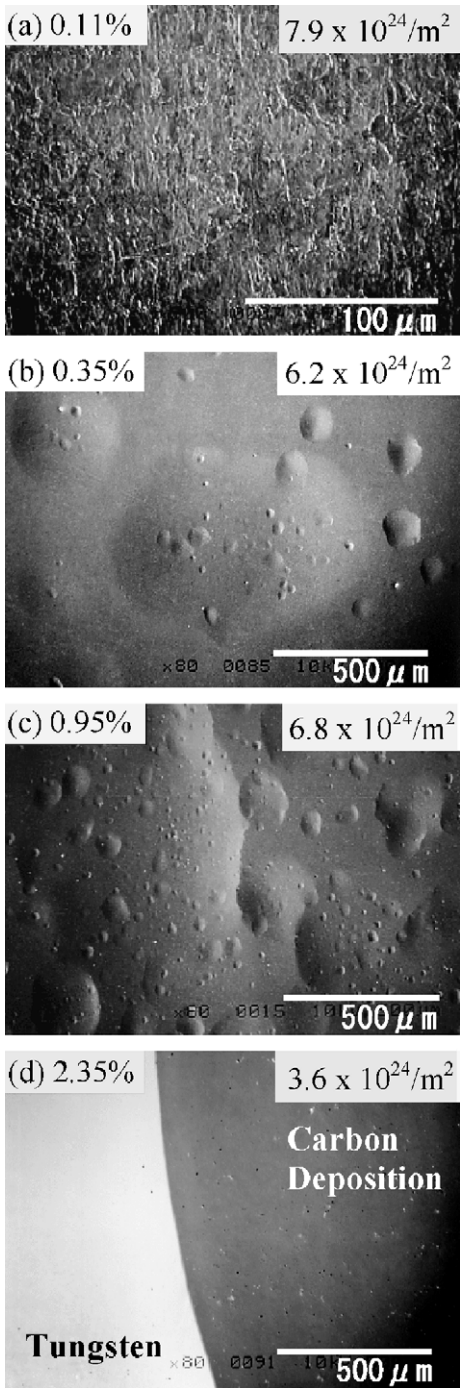

Fig. 3. SEM micrograph of the tungsten target after being irradiated by carbon and hydrogen mixed ion beam mainly with beam energy of 333 eV H and 1.0 keV C at 653 K. Carbon concentration was (a) 0.11%, (b) 0.35%, (c) 0.95%, (d) 2.35%.

From TRIM calculations [13] the implantation ranges of the hydrogen ions were estimated as 3–8 nm, and the implantation range of the carbon ions was estimated

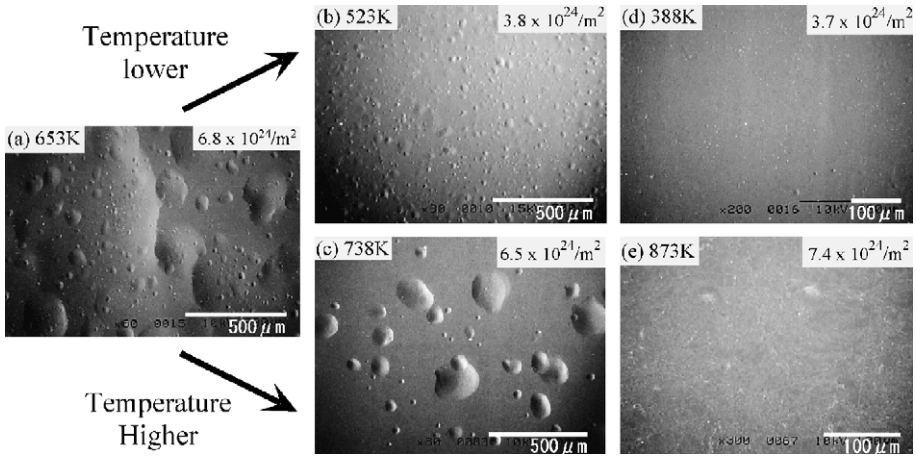

Fig. 4. SEM micrograph of the tungsten target after being irradiated by carbon and hydrogen mixed ion beam mainly with beam energy of 333 eV H and 1.0 keV C. Carbon concentration was 0.7–1.0%. Sample temperature was (a) 653 K, (b) 523 K, (c) 738 K, (d) 388 K, (e) 873 K.

as 2–4 nm. As a result, hydrogen would be implanted and diffuse deeper than the carbon. Retained carbon might react chemically with the tungsten and form a WC layer at or near the surface. XPS measurement detected the shifted C 1s peak (energy 283.1 eV) corresponding to WC over a depth of several hundred nm. Such a WC layer might act as a diffusion barrier because of low diffusivity in the WC layer [14,15], reducing the amount of hydrogen reaching the surface and being released. As a result, internal gas pressure by trapped hydrogen and build up at the vacancy or W/WC interface might deform the surface layer, and form blisters. It is also possible that implanted carbon diffuses beyond the ion range and creates defect sites at which hydrogen is trapped.

3.2. Sample temperature effect

In this series of experiments, the sample temperatures were varied from 388 to 873 K while the beam energy was fixed at 1.0 keV and the carbon concentration was maintained at 0.7–1.0%. With the sample at 653 K, the sizes and numbers of blisters were the largest (Fig. 4(a)). With the samples at 523 K (Fig. 4(b)) and 738 K (Fig. 4(c)), smaller blisters were observed. With the samples at 388 K (Fig. 4(d)) and 873 K (Fig. 4(e)), no blisters of size of 1.0 μm or greater were observed.

At the lowest temperature, hydrogen would not diffuse as far from the ion range as at higher temperatures. As a result, it may be that very small, high-pressure bubbles would be created in or near the implanted zone. These bubbles might collapse due to the formation of micro-cracks, releasing the hydrogen through the surface and preventing the growth of blisters.

At higher temperatures the hydrogen diffusivity increases and hydrogen could diffuse further into the sample possibly collecting at grain boundaries and dislocations. As a result, less hydrogen would be lost through micro-crack formation, and blisters could grow from the small bubbles.

At even higher temperature, faster diffusion would lead to lower hydrogen concentrations throughout the sample, both through dilution and through losses at surfaces. Also, trap sites might be emptied of hydrogen through thermal detrapping. As a result, there would not be hydrogen retained enough to form blisters.

If the flux and fluence were higher, the large blisters might occur even at higher sample temperature. For example, Ye et al., reported [16] that the blisters with size up to a few hundred μm were observed on tungsten surface by hydrogen ion irradiation at incident energy at 90 eV, the flux of an order of 10^{22} $m^{-2}\,s^{-1}$, the fluence higher than 1.4×10^{25} m^{-2}, and surface temperature of 920 K.

4. Conclusion

Blister formation in tungsten was studied by irradiating samples with mixed carbon and hydrogen ion beam with the beam ion energies were 1.0 keV and 300 eV, and the fluence was in the range of 10^{24}–10^{25} ions m^{-2}. The following conclusions were drawn;

(i) A small amount of carbon impurity in the ion beam had a large effect on blister formation. When the carbon concentration was 0.11%, there was little erosion, and no blisters of size of 1.0 μm or greater were observed. When the carbon concentration was more than 0.35%, a large number of blisters of various sizes were formed. When the carbon concentration was 2.35%, there was net deposition of carbon

by about 220 nm on the tungsten surface, leading to the growth of a carbon layer. No blisters were observed with this irradiation.

(ii) Sample temperature effect on blister formation was also investigated. The sample temperatures were varied from 388 to 873 K while the beam energy was fixed at 1.0 keV and the carbon concentration was maintained at 0.7–1.0%. With the sample at 653 K, the sizes and numbers of blisters were the largest. With the samples at 523 and 738 K, fewer and smaller blisters were observed. With the samples at 388 and 873 K, no blisters of size of 1.0 μm or larger were observed.

References

[1] G. Federici, C.H. Skinner, J.N. Brooks, J.P. Coad, C. Grisolia, A.A. Haasz, A. Hassanein, V. Philipps, C.S. Pitcher, J. Roth, W.R. Wampler, D.G. Whyte, Nucl. Fusion 41 (2001) 1967.
[2] D. Naujoks, W. Eckstein, J. Nucl. Mater. 220–222 (1995) 993.
[3] D. Naujoks, W. Eckstein, J. Nucl. Mater. 230 (1996) 93.
[4] A. Haasz, M. Poon, J.W. Davis, J. Nucl. Mater. 266–269 (1999) 520.
[5] W. Wang, J. Roth, S. Lindig, C.H. Wu, J. Nucl. Mater. 299 (2001) 124.
[6] T. Venhaus, T. Abeln, R. Doerner, R. Causey, J. Nucl. Mater. 290–293 (2001) 505.
[7] R.A. Causey, J. Nucl. Mater. 300 (2002) 91.
[8] F.C. Sze, R.P. Doerner, S. Luckhardt, J. Nucl. Mater. 264 (1999) 89.
[9] T. Shimada, T. Kawakami, Y. Ueda, A. Sagara, M. Nishikawa, J. Plasma Fusion Res. Ser. 3 (2000) 312.
[10] T. Shimada, Y. Ueda, A. Sagara, M. Nishikawa, Rev. Sci. Instrum. 73 (2002) 1741.
[11] Y. Ueda, H. Kikuchi, T. Shimada, A. Sagara, B. Kyoh, M. Nishikawa, Fusion Eng. Des. 61&62 (2002) 255.
[12] K. Krieger, J. Roth, J. Nucl. Mater. 290–293 (2001) 107.
[13] W. Eckstein, Computer Simulation of Ion–Solid Interaction, Springer Series in Material Science, vol. 10, Springer, Berlin, 1991.
[14] M. Poon, J.W. Davis, A.A. Haasz, J. Nucl. Mater. 283–287 (2000) 1062.
[15] V.Kh. Alimov, K. Ertl, J. Roth, K. Schmid, J. Nucl. Mater. 282 (2000) 125.
[16] M.Y. Ye, S. Fukuta, N. Ohno, S. Takamura, these Proceedings. PII: S0022-3115(02)01349-1.